Design of Part Feeding and Assembly Processes with Dynamics

Peng Song*, J. C. Trinkle†, Vijay Kumar‡, and Jong-Shi Pang§

*GRASP Lab, University of Pennsylvania, Philadelphia, PA 19104. Email: pengs@grasp.cis.upenn.edu
†Dept. of Computer Science, Rensselaer Polytechnic Institute, Troy, NY 12180. Email: trink@cs.rpi.edu
‡GRASP Lab, University of Pennsylvania, Philadelphia, PA 19104. Email: kumar@grasp.cis.upenn.edu
§Dept. of Mathematical Sciences, Rensselaer Polytechnic Institute, Troy, NY 12180. Email: pangj@rpi.edu

***Abstract*— We introduce a general methodology for the analysis and design of systems with multiple frictional contacts, with a specific focus on applications to part feeding and assembly processes. We derive computational support tools, especially dynamic models that underlie these models. We describe two dynamic models, the Stewart-Trinkle model [1] and an extension of the Song-Pang-Kumar model [2]. These models automate the process of identifying sufficing parameters and allow the designer to experiment with different configurations at the detailed design stage. Because the design process will be guided by analytical models, experimental observations can be easily integrated to refine these models allowing an efficient approach to redesign.**

I. Introduction

There are many manufacturing processes in which nominally rigid bodies undergo frictional contacts, possibly involving impacts. Examples of such processes include part-feeding, assembly, fixturing, material handling, and disassembly. In order to understand the complexity of such processes it is useful to consider the part orienting device shown in Figure 1. A cup-shaped part enters chute "A" in one of two nominal orientations, which we will call "open end up" (on the left) and "open end down" (on the right). The objective of this mechanism is to cause the part to exit chute "C" in the "open end up" configuration regardless of the orientation when entering chute "A". The part is subject to multiple frictional contacts with the walls of the chutes and the pin "B". It undergoes frictional impacts before either going down the chute or gets stuck inside the device. There are many factors that affect this feeding process, including the geometry and physical properties of the device and part and the part's initial condition. Typically, the preliminary design of such systems is based on strong intuition, and the detailed design is refined empirically via prototyping. If the prototype does not function properly, as is usually the case in the first several trials, there is no systematic approach to redesign, because the design constraints of such systems are dominated by unilateral constraints and constant transitions between contact states.

The dynamics of part feeding and assembly processes are notoriously difficult to predict because the dynamic models for systems with unilateral constraints are vastly inadequate, and in some cases, do not exist. This is true even for the case of deterministic models. In the past, geometric and quasi-static approaches have been adopted to planning manipulation [3], [4], [5], [6], assembly [7], [8], part feeding [9], fixturing [10], [11], and grasping tasks [12]. Only now are some of the fundamental underpinnings of systems with multiple frictional contacts and impacts being explored rigorously [13], [14], [15]. However, there is no systematic approach to planning/design in problems with dynamics [16].

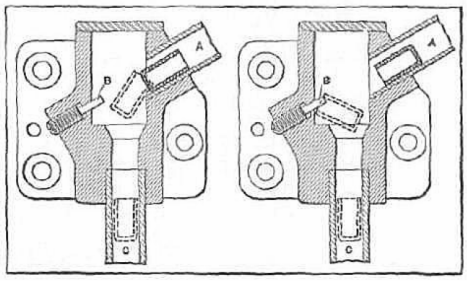

Fig. 1. The exit orientation of the cup-shaped part must be with the open end up, regardless of the entering orientation [17].

In this paper, we introduce a framework for design of part feeding and automated assembly processes. We also derive dynamic models and the optimization with parameters that underlie these models. We describe two dynamic models: the Stewart-Trinkle model [1], a linear complementary problem model that handles contact transitions and with an implicit assumption that impacts are inelastic; and an extension of the Song-Pang-Kumar model [2], a more general, nonlinear complementary model capable of approximating a wide variety of types of contact conditions including elastic or viscoelastic impacts. Numerical studies on both models are reported in Section IV. In Section V, we apply the Stewart-Trinkle model to the design of a part feeding mechanism described in Figure 1.

II. Design framework

The automatic assembly and part feeding systems can be modeled as switched systems, a special class of hybrid systems in which the state space can be partitioned into $n_Q \in Q$ non-overlapping regions, each corresponding to a mode of operation characterized by continuous dynamics. The system state in the figure is characterized by a *continuous state* $X \in \Re^n$ and a collection of *discrete modes* or discrete states. Each mode consists of a set of *ordinary differential equations* (ODEs) or *differential algebraic equations* (DAEs) that govern the evolution of the continuous state X and a set of *invariants* that describe the conditions under which the ODEs or DAEs

are valid. The continuous and discrete states are defined as $(X, Q) \in \mathcal{X} \times \mathcal{Q}$ where $\mathcal{X} \subset \Re^n$ and $\mathcal{Q}$ is the set of natural numbers, with $Q \in \mathcal{Q}$ denoting the Qth mode. $P \in \mathcal{P} \subset \Re^k$ is a set of time invariant parameters which appear in the model. These include the geometric parameters, the initial conditions, and the parameters related to the material properties, such as friction, restitution, stiffness, and damping. Exogenous inputs, disturbances and noise are not considered in this paper.

The differential equations in mode Q are given by:

$$\dot{X} = \mathcal{F}_Q(X, P) \tag{1}$$

Each mode Q corresponds to a particular assignment of contact conditions (rolling, sliding, or no contact) to each frictional contact. Thus, for a system with n_c potential contacts, there are 3^{n_c} possible discrete modes, each characterized by a set of conditions in state space. Figure 2 shows the schematic of a switched system with 6 modes. $\mathcal{F}$ represents the *dynamic model* that governs the continuous states X within each mode. The dynamic model may be difficult to obtain in practice. Further, $\mathcal{F}$ may not have a unique solution. Under such a circumstance, the representation of states partitions shown in Figure 2 may not be valid or may lead to multivalued solutions. In the next section, we will describe two discrete-time dynamic models. The method we use to develop these models is influenced by the extensive recent work on *complementarity problems* and *time-stepping models* for dynamic simulation of rigid-body systems [14], [18], [19].

III. Dynamic Models

The dynamic equation of motion for a multibody system with contact interactions can be written in the form

$$M(q)\dot{\nu} = u(t, q, \nu) + W_{\mathrm{n}}(q)\lambda_{\mathrm{n}} + W_{\mathrm{t}}(q)\lambda_{\mathrm{t}} + W_{\mathrm{o}}(q)\lambda_{\mathrm{o}}, \tag{2}$$

where q is the n_q-dimensional vector of generalized coordinates, ν is the n_ν-dimensional vector of the system velocities. $M(q)$ is the $n_\nu \times n_\nu$ symmetric positive definite inertia matrix, $u(t, q, \nu)$ is the n_ν-dimensional external force vector (excluding contact forces). For a system with n_c contacts, $\lambda_{\mathrm{n,t,o}}$ are the n_c-dimensional concatenations of the contact forces in the normal direction (labelled n) and the two tangential directions (labelled t and o), and $W_{\mathrm{n,t,o}}(q)$ are the $n_\nu \times n_c$ Jacobian matrices. The kinematics equations relate the system velocity ν to the time-derivative of the system configuration $\dot{q} \equiv dq/dt$ via a $n_q \times n_\nu$ parametrization matrix $G(q)$:

$$\dot{q} = G(q)\nu. \tag{3}$$

To complete the formulation of the model, we need to include the contact conditions. In the normal direction, the contact condition of the system is governed by

$$0 \le \lambda_{i\mathrm{n}} \perp \phi_{i\mathrm{n}} \ge 0, \quad i = 1 \dots n_c, \tag{4}$$

where $\perp$ denotes perpendicularity and $\phi_{i\mathrm{n}}$ is the normal separation between contacting objects at the ith contact.

In the tangential direction, the contact conditions are formulated by requiring that friction forces maximize the energy dissipation rate over the sets of admissible contact forces computed based on the friction model. For Coulomb's quadratic cone, the maximum dissipation principle for at the ith ($i = 1 \dots n_c$) contact can be written as

$$(\lambda_{i\mathrm{t}}, \lambda_{i\mathrm{o}}) = \operatorname{argmin} \{(s_{i\mathrm{t}}\lambda_{i\mathrm{t}} + s_{i\mathrm{o}}\lambda_{i\mathrm{o}} : (\lambda_{i\mathrm{t}}, \lambda_{i\mathrm{o}}) \in \mathcal{FC}(\mu_i\lambda_{i\mathrm{n}})\}$$

where $$\mathcal{FC}(\mu_i\lambda_{i\mathrm{n}}) \equiv \left\{(\lambda_{i\mathrm{t}}, \lambda_{i\mathrm{o}}) : \sqrt{\lambda_{i\mathrm{t}}^2 + \lambda_{i\mathrm{o}}^2} \le \mu_i\lambda_{i\mathrm{n}}\right\}, \tag{5}$$

and s_i represent the slip velocities at the ith contact. The Coulomb's cone is not differentiable at the origin where $\lambda_{i\mathrm{n}} = 0$ or $\mu_i = 0$. We introduce the following smooth cone to resolve this problem:

$$\mathcal{FC}_\gamma(\mu_i\lambda_{i\mathrm{n}}) \equiv \left\{(\lambda_{i\mathrm{t}}, \lambda_{i\mathrm{o}}) : \sqrt{\lambda_{i\mathrm{t}}^2 + \lambda_{i\mathrm{o}}^2 + \gamma^2} \le \mu_i\lambda_{i\mathrm{n}} + \gamma\right\} \tag{6}$$

where $\gamma \ge 0$ is a small scalar. When $\gamma = 0$, the smooth cone (6) converges to the Coulomb's quadratic cone (5) with the assumption that $0/0 \equiv 0$. Note that the smooth cone preserves all the properties of the Coulomb's quadratic cone.

However, even for the smooth cone, there is no suitable *constraint qualification* for the KKT conditions when the contact is inactive ($\lambda_{i\mathrm{n}} = 0$) or when the contact is frictionless ($\mu_i = 0$). To obtain the optimality conditions, we resort to the Fritz John conditions[1].

$$\begin{aligned}
0 \;\le\; \beta_i \;\perp\; \mu_i\lambda_{i\mathrm{n}} + \gamma - \sqrt{\lambda_{i\mathrm{t}}^2 + \lambda_{i\mathrm{o}}^2 + \gamma^2} \;&\ge\; 0 \\
\beta_{i0}s_{i\mathrm{t}} \;+\; \frac{\beta_i\lambda_{i\mathrm{t}}}{\sqrt{\lambda_{i\mathrm{t}}^2 + \lambda_{i\mathrm{o}}^2 + \gamma^2}} \;&=\; 0 \\
\beta_{i0}s_{i\mathrm{o}} \;+\; \frac{\beta_i\lambda_{i\mathrm{o}}}{\sqrt{\lambda_{i\mathrm{t}}^2 + \lambda_{i\mathrm{o}}^2 + \gamma^2}} \;&=\; 0 \\
\beta_{i0} \;\ge\; 0\,, \quad (\beta_{i0}\ \beta_i) \;&\neq\; 0
\end{aligned} \tag{7}$$

If $\beta_{i0} \neq 0$, the KKT conditions hold (with the Lagrange multipliers being defined as $\hat{\beta}_i \equiv \beta_i/\beta_{i0}$). In a contact problem, we can use $\mu_i\lambda_{i\mathrm{n}}$ as a natural choice for β_{i0} instead of solving for the extra multiplier. When $\mu_i\lambda_{i\mathrm{n}} = 0$, the Fritz John conditions can be trivially satisfied with a nonzero β_i. These conditions will be used in the next subsection to extend the traditional complementarity conditions to include both active and inactive contact constraints.

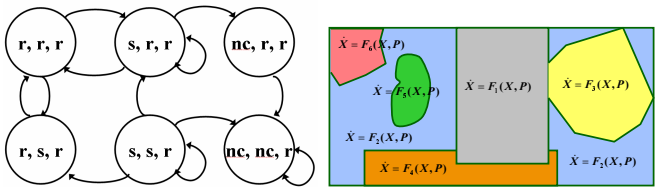

(a) Contact state representation for a system with three contacts (r–rolling; s–sliding; nc–no contact).

(b) The switched dynamical system representation corresponding to the contact states representation above.

Fig. 2. The dynamic equations of motion change as the contact state changes making the resulting time history non smooth.

[1]See [20] (Chapters 4 and 5) for details on KKT conditions, Fritz John conditions, and constraint qualifications.

The Coulomb's quadratic cone can be linearized using the following polyhedra approximation, at any $i = 1 \dots n_c$:

$$\widehat{\mathcal{FC}}(\mu_i \lambda_{\mathrm{in}}) \equiv \{D_i \lambda_{\mathrm{if}} : \|\lambda_{\mathrm{if}}\|_1 \leq \mu_i \lambda_{\mathrm{in}}, \lambda_{\mathrm{if}} \succcurlyeq 0\} \tag{8}$$

where D_i is a $2 \times n_l$ matrix whose columns are coplanar vectors $d_{i,j},\ j = 1, \dots n_l$ in the plane tangent to the contact normal (the t-o plane) and n_l is the number of edges of the polyhedra. The jth component of λ_{if} represents the magnitude of tangential force along the $d_{i,j}$ direction. The polyhedra approximation leads to a linearly constrained problem, thus automatically satisfies the Abadie constraint qualification for the KKT conditions [20]. The following complementarity conditions can be derived from the the maximum dissipation principle problem as :

$$\begin{array}{rcccccl} 0 & \leq & \beta_i e_i \ + \ D_i^T s_i & \perp & \lambda_{\mathrm{if}} & \geq & 0 \\ 0 & \leq & \mu_i \lambda_{\mathrm{in}} - e_i^T \lambda_{\mathrm{if}} & \perp & \beta_i & \geq & 0 \end{array}, \tag{9}$$

wheree_i is a n_l-vector of ones.

Together, (2), (3), (4), and (7) or (9) constitute the equations of motion which have four components: the dynamics of the mechanical system, the kinematic map, the normal contact conditions, and the friction law.

We consider a time discretization of the differential equations (2) and (3) for $t \in (0, T]$. Fix a positive integer N and let $h \equiv T/N$. Partition the interval $[0, T]$ into N subintervals $[t_\ell, t_{\ell+1}]$, where $t_\ell \equiv \ell h$, for $\ell = 0, 1, \dots, N$. Write

$$q^\ell \equiv q(t_\ell), \quad \nu^\ell \equiv \nu(t_\ell), \quad \text{and} \quad \lambda^\ell_{\mathrm{n,t,o}} \equiv \lambda_{\mathrm{n,t,o}}(t_\ell).$$

The time derivatives $\dot{\nu}$ and $\dot{q}$ are replaced by the backward Euler approximations: for all $\ell = 0, \dots, N-1$,

$$\dot{\nu}(t_{\ell+1}) \approx \frac{\nu^{\ell+1} - \nu^\ell}{h} \quad \text{and} \quad \dot{q}(t_{\ell+1}) \approx \frac{q^{\ell+1} - q^\ell}{h}.$$

The various time-stepping schemes differ in how $M(q)$ and the right-hand sides in (2) and (3) are approximated.

In the *fully implicit scheme*, all functions are evaluated at time $\ell+1$. Because the variables such as the inertia matrix and the Jacobians are functions of $q^{\ell+1}$, solving for the unknowns $q^{\ell+1}$ and $\lambda^{\ell+1}$ involves the solution of nonlinear equations. In contrast, a *semi-implicit* scheme may lead to a linear formulation in terms of $q^{\ell+1}$, $\nu^{\ell+1}$, and $\lambda^{\ell+1}$ at the ℓth time step.

A. A semi-implicit method for rigid contacts with inelastic collisions

Stewart and Trinkle [1] developed a semi-implicit time-stepping model that was originally formulated as a mixed LCP in terms of the unknown state $(\nu^{\ell+1}, q^{\ell+1})$, normal and frictional impulses $(p_{\mathrm{n}}^{\ell+1}, p_{\mathrm{f}}^{\ell+1})$ (defined as: $p_{\mathrm{n}}^{\ell+1} = h\lambda_{\mathrm{n}}^{\ell+1}$, $p_{\mathrm{f}}^{\ell+1} = h\lambda_{\mathrm{f}}^{\ell+1}$), and slack variable $\beta^{\ell+1}$ approximating the magnitude of the sliding velocity at the contact. However, the state variables can be eliminated by using the equations of motion, thus allowing reformulation of the time-stepping method as a standard LCP(B, b) written as follows:

$$w^{\ell+1} = B^\ell z^{\ell+1} + b^\ell \tag{10}$$

$$0 \leq w^{\ell+1} \perp z^{\ell+1} \geq 0 \tag{11}$$

with B^ℓ, b^ℓ, and $z^{\ell+1}$ given as follows:

$$B^\ell = \begin{pmatrix} W_{\mathrm{n}}^T M^{-1} W_{\mathrm{n}} & W_{\mathrm{n}}^T M^{-1} W_{\mathrm{f}} & 0 \\ W_{\mathrm{f}}^T M^{-1} W_{\mathrm{n}} & W_{\mathrm{f}}^T M^{-1} W_{\mathrm{f}} & E \\ U & -E^T & 0 \end{pmatrix} \tag{12}$$

$$b^\ell = \begin{pmatrix} W_{\mathrm{n}}^T (\nu + M^{-1} u h) + \phi_{\mathrm{n}}(q^\ell)/h \\ W_{\mathrm{f}}^T (\nu + M^{-1} u h) \\ 0 \end{pmatrix}, \ z^{\ell+1} = \begin{pmatrix} p_{\mathrm{n}}^{\ell+1} \\ p_{\mathrm{f}}^{\ell+1} \\ \beta^{\ell+1} \end{pmatrix} \tag{13}$$

where E is a block diagonal matrix, with each diagonal block equal to a column vector length n_l with all elements equal to one. U has the same structure as E with all elements of the diagonal block equal to μ_i, the coefficient of friction at contact point i. Note that this LCP is only linear because all quantities in B and b are computed at time t^ℓ.

Several points are worth noting. First, the term $\phi_{\mathrm{n}}(q^\ell)/h$ provides constraint stabilization with $\phi_{\mathrm{n}}(q^\ell)$ being the vector of the normal separations between each pair of bodies in or about to be in contact. When it is negative (implying inter-penetration of bodies), it acts to generate a bias impulse that increases the normal component of the relative velocity at a contact be large enough to eliminate the penetration at the end of the next time step. Second, there is no restitution law built into this formulation. To include realistic bouncing effects, one must stop the ST method at the time of each collision and apply an impact model such as Newton's, Poisson's, or Stronge's hypothesis. The usual quadratic friction cone and nonpenetration constraints have been linearized in order to obtain a LCP. Fourth, the quantities (such as M and W_n) not superscripted with a time index are assumed to be functions of the known state, (ν^ℓ, q^ℓ). Otherwise, as stated above, the LCP would become a nonlinear complementarity problem (NCP).

B. A fully-implicit method with visco-elastic contacts

Song, Kumar, and Pang [2] developed a discrete-time compliant contact model for rigid body simulation. The key idea of this model is to allow local compliance at the contact patch between nominally rigid bodies. Unlike some penalty methods, the compliant model relies on both normal and tangential compliances to model contact forces and can resolve the inconsistencies with uniqueness and existence. In this subsection, we extend the model using a fully implicit time-stepping scheme. The extended model will lead to unified framework for simulation of systems with sustained contacts as well as impacts. We will use a lumped viscoelastic model for contact forces, which is a special case of the distributed compliant model described in [2]. For the lumped model, at each *potential* contact point i ($i = 1, \dots, n_c$), we have the following decoupled relations between the contact force λ and the local deformation δ, in the n, t, and o directions respectively:

$$\lambda_{i\,\mathrm{n,t,o}} = K_{i\,\mathrm{n,t,o}}\, \delta_{i\,\mathrm{n,t,o}} + C_{i\,\mathrm{n,t,o}}\, \dot{\delta}_{i\,\mathrm{n,t,o}}. \tag{14}$$

In the compliant model, the normal separation ϕ_{in} and the tangential slip velocities $s_{\mathrm{it,o}}$ are affected by both the rigid

body gross motion and the local deformations:

$$\phi_{i\mathrm{n}}(q) \equiv \delta_{i\mathrm{n}} + \Psi_{i\mathrm{n}}(q), \quad (15)$$

$$s_{i\mathrm{t,o}} \equiv \dot{\delta}_{i\mathrm{t,o}} + W_{i\mathrm{t,o}}^T(q)\nu, \quad (16)$$

where $\Psi_{i\mathrm{n}}$ denotes separation caused by the rigid gross motion and $W_{i\mathrm{t,o}}$ the ith columns of W_{t} or W_{o}. Note that for rigid body models, $\phi_{i\mathrm{n}} \equiv \Psi_{i\mathrm{n}}$ since $\delta_{i\mathrm{n}} \equiv 0$ at a perfectly rigid contact. Writing

$$\delta_{i\,\mathrm{n,t,o}}^{\ell} \equiv \delta_{i\,\mathrm{n,t,o}}(t_\ell), \quad \ell = 0, 1, \ldots, N,$$

together with the fully implicit discretization of system dynamics equations (2,3) and the contact constraints (4, 7, 14-16) for all $i = 1 \ldots n_c$, we have the following discrete-time, mixed nonlinear complementarity problem formulation for dynamics of systems with unilateral constraints:

$$\begin{aligned}
\nu^{\ell+1} &= \nu^{\ell} + hM(q^{\ell+1})^{-1}u^{\ell+1} + hM(q^{\ell+1})^{-1} \cdot \\
&\quad \left[W_{\mathrm{n}}(q^{\ell+1})\lambda_{\mathrm{n}}^{\ell+1} + W_{\mathrm{t}}(q^{\ell+1})\lambda_{\mathrm{t}}^{\ell+1} + W_{\mathrm{o}}(q^{\ell+1})\lambda_{\mathrm{o}}^{\ell+1}\right] \\
q^{\ell+1} &= q^{\ell} + hG(q^{\ell+1})\nu^{\ell+1} \\
0 \le \lambda_{i\mathrm{n}}^{\ell+1} &\perp \phi_{i\mathrm{n}}(q^{\ell+1}) \ge 0 \\
\phi_{i\mathrm{n}}(q^{\ell+1}) &= \delta_{i\mathrm{n}}^{\ell+1} + \Psi_{i\mathrm{n}}(q^{\ell+1}) \\
0 \le \beta_i^{\ell+1} &\perp \mu\lambda_{i\mathrm{n}}^{\ell+1} + \gamma - \sqrt{\left(\lambda_{i\mathrm{t}}^{\ell+1}\right)^2 + \left(\lambda_{i\mathrm{o}}^{\ell+1}\right)^2 + \gamma^2} \ge 0 \\
\mu\lambda_{i\mathrm{n}}^{\ell+1} s_{i\mathrm{t,o}}^{\ell+1} &= -\frac{\beta_i^{\ell+1}\lambda_{i\mathrm{t,o}}^{\ell+1}}{\sqrt{\left(\lambda_{i\mathrm{t}}^{\ell+1}\right)^2 + \left(\lambda_{i\mathrm{o}}^{\ell+1}\right)^2 + \gamma^2}} \\
s_{i\mathrm{t,o}}^{\ell+1} &= \frac{\delta_{i\mathrm{t,o}}^{\ell+1} - \delta_{i\mathrm{t,o}}^{\ell}}{h} + W_{i\mathrm{t,o}}^T(q^{\ell+1})\nu^{\ell+1} \\
\lambda_{i\,\mathrm{n,t,o}}^{\ell+1} &= \left(K_{i\,\mathrm{n,t,o}} + \frac{1}{h}C_{i\,\mathrm{n,t,o}}\right)\delta_{i\,\mathrm{n,t,o}}^{\ell+1} - \frac{1}{h}C_{i\,\mathrm{n,t,o}}\delta_{i\,\mathrm{n,t,o}}^{\ell}
\end{aligned} \quad (17)$$

As an example, we apply the NCP model (17) to the simulation of a rough spherical body bouncing and rolling on the ground. Depending on the material properties of the contacting rigid bodies, the ball can undergo one or more frictional impacts and end up in a condition in which it maintains contact with the ground. The model (17) is a unified approach to incorporating all these conditions. The generalized coordinates and the system velocities are given by

$$\begin{aligned}
q &= (\,x \quad y \quad z \quad e_0 \quad e_x \quad e_y \quad e_z\,)^T \\
\nu &= (\,\nu_x \quad \nu_y \quad \nu_z \quad \omega_x \quad \omega_y \quad \omega_z\,)^T
\end{aligned}$$

where (x, y, z) are the Cartesian coordinates of the center of mass, (e_0, e_x, e_y, e_z) are the Euler parameters, (ν_x, ν_y, ν_z) are the linear velocities along the Cartesian axes, and $(\omega_x, \omega_y, \omega_z)$ are the angular velocities.

The initial conditions of the object are given by

$$\begin{aligned}
q^0 &= (\,0 \quad 0 \quad 0.2 \quad 1 \quad 0 \quad 0 \quad 0\,)^T \\
\nu^0 &= (\,0.5 \quad 0 \quad 0 \quad 20 \quad 0 \quad 0\,)^T .
\end{aligned}$$

The effective coefficient of restitution for impact for this example is approximately 0.8. An empirical expression of the coefficient of restitution for impacts with the compliant contact model can be found in [21]. The NCP is solved by using the AMPL/PATH solver [22] on the NEOS server for optimization at the Argonne National Laboratory. The snapshots of the simulation results and the top view of the motion history at the center of mass are plotted in Figure 3.

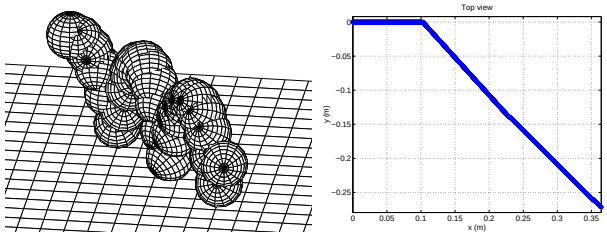

Fig. 3. The trajectory of a rough spherical body with frictional impacts. The object is launched with an initial velocity of 0.5m/s in the x-direction at a height of 0.2m above the horizontal plane and a spin velocity of 20rad/sec around the x-axis. The mass of the ball is $m = 0.2$kg and the radius is $r = 0.05$m. Other parameters in model (17) include $h = 2 \times 10^{-4}$sec, $N = 5000$, $\gamma = 10^{-8}$, $K = 5 \times 10^4$N/m, and $C = 2\sqrt{K}$sec·N/m.

IV. Frictional Impacts

In this section we use the simple example of a rectangular, planar object impacting a horizontal plane to illustrate the modeling of frictional impacts. In this example, there are four potential contacts between the block and the horizontal plane. The maximum number of contact state transitions are 3^4, most of which are geometrically infeasible.

The generalized coordinates of the peg are given by

$$q = (\,x \quad y \quad \theta\,)^T \quad \text{and} \quad \nu = (\,\dot{x} \quad \dot{y} \quad \dot{\theta}\,)^T ,$$

where (x, y) are the coordinates of the center of mass, and θ is the orientation of the peg. Other than the contact forces, gravity is the only external force acting on the peg.

$$M(q) = \begin{pmatrix} m & 0 & 0 \\ 0 & m & 0 \\ 0 & 0 & J \end{pmatrix}, \; G(q) = I_{3\times 3}$$

$$W_{i\mathrm{n}}(q) = \begin{pmatrix} 0 \\ 1 \\ x_{vi}(q) - q(1) \end{pmatrix}, \; W_{i\mathrm{t}}(q) = \begin{pmatrix} 1 \\ 0 \\ q(2) - y_{vi} \end{pmatrix}$$

where $(x_{vi},\ y_{vi})$ are the coordinates of the ith vertex, $i = 1 \ldots 4$. The initial conditions of the peg are set as:

$$q_0 = (\,0 \quad 0.2 \quad \pi/4\,)^T \quad \text{and} \quad \nu_0 = (\,0 \quad 0 \quad 0\,)^T .$$

We are able to observe both the elastic impact and inelastic impact effect if we increase the damping ratio of the local compliance at the contact. The snapshots of the simulation results are shown in Figures 4 and 5.

V. Design of the Part Feeding Mechanism

Figure 6 shows a reorienting mechanism with 12 design variables. The variables are as follows:

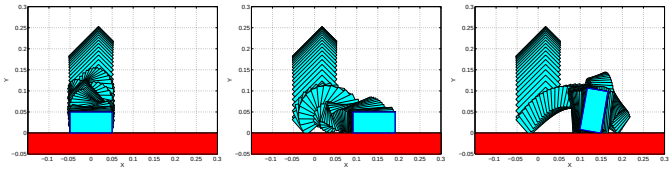

Fig. 4. Simulation of impacts between a rectangular peg and the horizontal plane with three different friction coefficients: $\mu = 0$ (left), $\mu = 0.2$ (middle), and $\mu = 1.0$ (right). The peg is released from still at a distance of 0.2m between the center of mass and the horizontal plane. The mass of the peg is $m = 0.2$kg and the inertia $J = 2 \times 10^{-4}\text{kg} \cdot \text{m}^2$. Other parameters used in this example are given as $h = 2 \times 10^{-4}$sec, $N = 5000$, $\gamma = 10^{-8}$, $K = 5 \times 10^4$N/m, and $C = 2\sqrt{K}$sec·N/m.

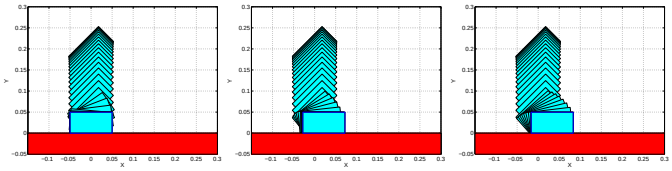

Fig. 5. Inelastic impacts can be predicted by model (17) if we increase the damping ratio to $C = 200 * \sqrt{K}$sec·N/m for the same three cases shown in Figure 4

a	width of input chute
b	width of output chute
c	depth of chamfer
d	length of input chute
e	horizontal location of left cavity wall
f	position of center of tip of protuberance
g	position of lower left corner of chute
r	radius of protuberance
θ	angle of input chute
α	angle of chamfer

Given a rectangular peg of fixed dimensions, mass, and moment of inertia, the goal was to determine the design parameters such that a peg entering with different orientations (as shown in Figure 7 and Figure 8) would always exit in the orientation with the center of gravity down. A secondary objective was to have the peg pass through the device quickly.

Let q_{goal} be a target configuration of the peg at some point well within the exit chute. Further, let T be the time when the peg either comes to rest or when the y component of its center of gravity moves below that of q_{goal}. The design problem was expressed as an optimization problem with the design space specified by simple bounds placed on the 12 design variables and the objective function given as follows:

$$\mathcal{G} = \sum_{i=1}^{2} w \, ||q_i(T_i) - q_{\text{goal}}|| + T_i \tag{18}$$

where w is a weight factor and $i \in \{1, 2\}$ with 1 or 2 indicating that the peg entered the input chute with center of gravity on the left or right. With this objective function, the design problem can be written as

$$P = \min_{P} \mathcal{G}(X, T) \quad \text{s.t. } \dot{X} = \mathcal{F}_Q(X, P), \tag{19}$$

where the parameter set P is the set of all the 12 design variables given at the beginning of this section, the states variable $X \equiv (q, \dot{q})$. In this design example, we use the ST model to compute $\mathcal{F}_{\mathcal{Q}}$ where Q represents the contact state set excluding the transitions from sustained contact to no contact. The objective function will be minimized when the peg fall through the device quickly and properly oriented.

The design was carried out in Matlab using the constrained optimization routine, `fmincon`, with the ST time-stepping method called twice for each objective function evaluation. The initial guess for the design is shown in Figures 7 and 8. Note that the peg comes to rest on the protrusion for both entering orientations.

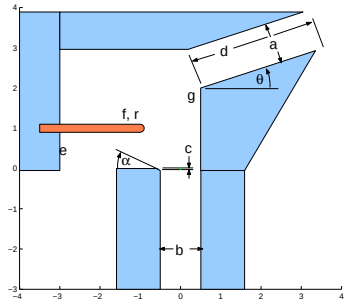

Fig. 6. Reorienting device with design variables taking on their initial values.

Figures 9 and 10 show the result obtained after approximately 1000 objective function evaluations. The weight factor w in the objective function is set to be 5. Note that the peg falls through the device in the proper orientation regardless of its entering orientation.

VI. Discussion

The problem of finding the feasible sets of design parameters and initial conditions for the assembly or part feeding processes is similar to *motion planning problem* in robotics where the goal is, given a robot with dynamics and constraints (obstacles), to find a path or trajectory (if exists) from the starting configuration to the goal configuration. Just as complete motion planning is hard to obtain for complex problems, we may not be able to develop complete algorithms, or prove correctness or safety. However, the challenge here is to develop a tractable algorithm that can be used for optimization of a system with nonsmooth dynamics in a nonconvex domain.

We described two time-stepping models that can be applied to simulation and design with dynamics. Both models can be used to solve the initial value problem that serves as the basis for the design optimization process as discussed in Section V. The ST model is more efficient computationally, because it leads to an LCP formulation, but if suffers from the implicit assumption of inelastic impacts. To incorporate elastic impacts, one stops the ST model at the time of the impact, applies an impact model, resets the velocity variables, and resumes time stepping. In contrast, the SPK model incorporates elastic impacts but is formulated as an NCP, which is difficult to solve.

If we replace the initial value problem in our design approach with a boundary value problem and impose the

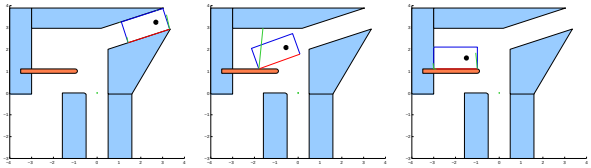

Fig. 7. Peg not able to pass through the device with initial design parameters with center of gravity starting on the right.

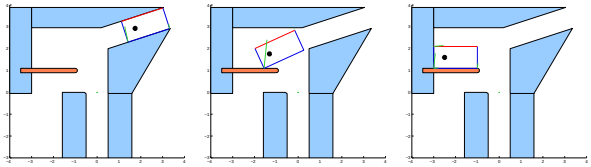

Fig. 8. Peg not able to pass through the device with initial design parameters with center of gravity starting on the left.

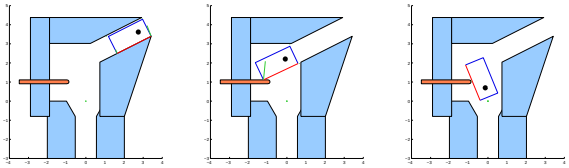

Fig. 9. Peg able to pass through the device with optimal design parameters with center of gravity starting on the right.

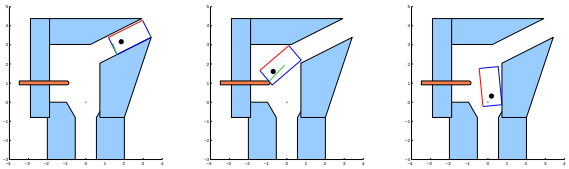

Fig. 10. Peg able to pass through the device with optimal design parameters with center of gravity starting on the left.

constraints of proper device function as part of the boundary conditions, we may be able to obtain a dynamically feasible design directly by solving a large boundary value problem. Unlike its initial-value counterpart, the boundary value problem is considerably more complicated. For one thing, it is no longer possible to decouple the time-stepping process into a finite sequence of individual subproblems each pertaining to a single time step. Therefore, model switching based on state monitoring is no longer available. Instead, one has to consider the entire system along with the boundary conditions as a large-scale mixed complementarity problem. A unified formulation becomes necessary in order to deal with all types of contact transitions without switching models. The SPK model is, to the authors' knowledge, the only existing discrete model that fits into this category. Investigation of design by solving the boundary value problem based on the SPK model will be addressed in a forthcoming paper.

ACKNOWLEDGEMENT

The authors thank Michael Ferris for providing and supporting PATH and Todd Munson for his help on improving the AMPL/PATH input for the NCP model (17). This work is based on research supported by the National Science Foundation under Grants DMS-0139715 and DMS-0139701.

REFERENCES

[1] D. Stewart and J. Trinkle, "An implicit time-stepping scheme for rigid-body dynamics with inelastic collisions and coulomb friction," *International Journal of Numerical Methods in Engineering*, vol. 39, pp. 2673–2691, 1996.

[2] P. Song, J.-S. Pang, and V. Kumar, "A semi-implicit time-stepping model for frictional compliant contact problems," International Journal for Numerical Methods in Engineering, to appear, 2003.

[3] S. Akella, W. Huang, K. Lynch, and M. Mason, "Sensorless parts feeding with a one joint robot," in *Workshop on the Algorithmic Foundations of Robotics*, 1996.

[4] J. Trinkle and J. J. Hunter, "A framework for planning dexterous manipulation," in *Proceedings of the 1991 IEEE International Conference on Robotics and Automation*, Apr. 1991, pp. 1245–1251.

[5] J. Trinkle and D. Zeng, "Prediction of the quasistatic planar motion of a contacted rigid body," *IEEE Transactions on Robotics and Automation*, vol. 11, no. 2, pp. 229–246, Apr. 1995.

[6] N. Zumel and M. Erdmann, "Nonprehensible two palm manipulation with non-equilbrium transitions between stable states," in *Proceedings of the 1996 IEEE International Conference on Robotics and Automation*, Apr. 1996, pp. 3317–3323.

[7] B. R. Donald and D. K. Pai, "On the motion of compliantly connected rigid bodies in contact: a system for analyzing designs for assembly," in *Proceedings of the 1990 IEEE International Conference on Robotics and Automation*, 1990, pp. 1756–1762.

[8] D. Balkcom and J. Trinkle, "Computing wrench cones for planar rigid body contact tasks," *The International Journal of Robotics Research*, vol. 21, no. 12, pp. 1053–1066, 2002.

[9] B. Mirtich, Y. Zhuang, K. Goldberg, J. Craig, R. Zanutta, B. Carlisle, and J. Canny, "Estimating pose statistics for robotic part feeders," in *Proceedings of the 1996 IEEE International Conference on Robotics and Automation*, 1996, pp. 1140–1146.

[10] J. D. Wolter and J. Trinkle, "Automatic selection of fixture points for frictionless assemblies," in *Proceedings of the 1994 IEEE International Conference on Robotics and Automation*, vol. 1, May 1994, pp. 528–534.

[11] T. Zhang and K. Goldberg, "Gripper point contacts for part alignment," *IEEE Transactions on Robotics and Automation*, vol. 18, no. 6, pp. 902–910, 2002.

[12] M. Cherif and K. Gupta, "Planning quasi-static motions for reconfiguring objects with a multi-fingered robotic hand," in *Proceedings of the 1997 IEEE International Conference on Robotics and Automation*, April 1997.

[13] B. Brogliato, *Nonsmooth Impact Mechanics - Models, Dynamics, and Control*. London: Springer-Verlag, 1996, lecture Notes in Control and Information Sciences.

[14] D. Stewart, "Rigid-body dynamics with friction and impact," *SIAM Review*, vol. 42, pp. 3–39, 2000.

[15] J. Trinkle, J.-S. Pang, S. Sudarsky, and G. Lo, "On dynamic multi-rigid-body contact problems with coulomb friction," *Zeitschrift für Angewandte Mathematik und Mechanik*, vol. 77, no. 4, pp. 267–280, 1997.

[16] K. Lynch, "Nonprehensile manipulation: Mechanics and planning," Ph.D. dissertation, School of Computer Science, Carnegie Mellon University, Mar. 1996.

[17] G. Boothroyd and A. H. Redford, *Mechanized Assembly: Fundamentals of parts feeding, orientation, and mechanized assembly*. London: McGraw-Hill, 1968.

[18] M. Anitescu and F. A. Potra, "A time-stepping method for stiff multibody dynamics with contact and friction," *International Journal of Numerical Methods in Engineering*, vol. 55, no. 7, pp. 753–784, 2002.

[19] J. Trinkle, J. Tzitzouris, and J.-S. Pang, "Dynamic multi-rigid-systems with concurrent distributed contacts," *The Royal Society Philosophical Transactions: Mathematical, Physical and Engineering Sciences*, vol. 359, pp. 2575–2593, 2001.

[20] M. S. Bazaraa and C. M. Shetty, *Nonlinear Programming: Theory and Algorithms*. New York: John Wiley & Sons, 1979.

[21] P. R. Kraus, A. Fredriksson, and V. Kumar, "Modeling of frictional contacts for dynamic simulation," in *Proceedings of IROS 1997 Workshop on Dynamic Simulation: Methods and Applications*, 1997.

[22] M. C. Ferris, R. Fourer, and D. M. Gay, "Expressing complementarity problems and communicating them to solvers," *SIAM Journal on Optimization*, vol. 9, pp. 991–1009, 1999.